



HAL
open science

Type II photosensitized oxidation in senescent microalgal cells at different latitudes: Does low under-ice irradiance in polar regions enhance efficiency?

Jean-Francois Rontani, Rémi Amiraux, Lukas Smik, Stuart Wakeham, Aurélien Paulmier, Frédéric Vaultier, Ha Sun-Yong, Min Jun-Oh, Simon Belt

► **To cite this version:**

Jean-Francois Rontani, Rémi Amiraux, Lukas Smik, Stuart Wakeham, Aurélien Paulmier, et al.. Type II photosensitized oxidation in senescent microalgal cells at different latitudes: Does low under-ice irradiance in polar regions enhance efficiency?. *Science of the Total Environment*, 2021, 779, pp.146363. 10.1016/j.scitotenv.2021.146363 . hal-03424281

HAL Id: hal-03424281

<https://hal.science/hal-03424281>

Submitted on 18 Nov 2021

HAL is a multi-disciplinary open access archive for the deposit and dissemination of scientific research documents, whether they are published or not. The documents may come from teaching and research institutions in France or abroad, or from public or private research centers.

L'archive ouverte pluridisciplinaire **HAL**, est destinée au dépôt et à la diffusion de documents scientifiques de niveau recherche, publiés ou non, émanant des établissements d'enseignement et de recherche français ou étrangers, des laboratoires publics ou privés.

1
2 Type II photosensitized oxidation in senescent microalgal cells
3 at different latitudes: Does low under-ice irradiance in polar
4 regions enhance efficiency?
5

6 Rontani Jean-François^{1*}, Amiraux Rémi^{1,2,3}, Smik Lukas⁴, Wakeham Stuart G.⁵,
7 Paulmier Aurélien⁶, Vaultier Frédéric¹, Ha Sun-Yong⁷, Min Jun-oh^{7,8}, Belt
8 Simon T.⁴
9

10 ¹ Aix Marseille Université, Université de Toulon, CNRS/INSU/IRD, Mediterranean Institute of
11 Oceanography (MIO), UM 110, 13288 Marseille, France.

12 ² Takuvik Joint International Laboratory, Laval University (Canada) - CNRS, Département
13 de biologie, Université Laval, Québec G1V 0A6, Québec, Canada.

14 ³ UMR 6539 Laboratoire des Sciences de l'Environnement Marin (CNRS, UBO, IRD,
15 Ifremer) Institut Universitaire Européen de la Mer (IUEM) Plouzané, France

16 ⁴ Biogeochemistry Research Centre, School of Geography, Earth and Environmental
17 Sciences, University of Plymouth, Drake Circus, Plymouth, Devon PL4 8AA, UK.

18 ⁵ Skidaway Institute of Oceanography, Savannah, Georgia, USA.

19 ⁶ Laboratoire d'Etudes en Géophysique et Océanographie Spatiales (LEGOS),
20 IRD/CNRS/UPS/CNES, Université de Toulouse, 31401 Toulouse Cedex 9, France.

21 ⁷ Division of Ocean Sciences, Korea Polar Research Institute, 26 Songdomirae-ro, Incheon, 21990,
22 Republic of Korea.

23 ⁸ Department of Marine Science and Convergence Technology, Hanyang University, 55
24 Hanyangdaehak-ro, Ansan, 15588, Republic of Korea.

25
26
27
28 * Corresponding author. Tel.: +33-4-86-09-06-02; fax: +33-4-91-82-96-41. E-mail address:
29 jean-francois.rontani@mio.osupytheas.fr (J.-F. Rontani)

30
31
32
33
34
35
36
37
38
39
40
41
42
43
44
45

Abstract

Comparison of Type II photosensitized oxidation of lipids (the photodynamic effect) and photodegradation of chlorophyll (sensitizer photobleaching) in samples of particulate matter collected previously from locations representing a diverse range of latitudes reveals an enhancement of the photooxidation of lipids at the expense of chlorophyll photodegradation in the polar regions. The efficiency of the photodynamic effect appears to be particularly high in sinking particles collected under sea ice and is attributed to the rapid settling of highly aggregated sympagic algae to depths of low light transmission favouring the photodynamic effect at the expense of photobleaching of the sensitizer. Paradoxically, the low efficiency of Type II photosensitized oxidation of lipids observed in temperate and equatorial regions is associated with high solar irradiances in these regions. Type II photosensitized oxidation of lipids in senescent phytoplankton seems thus to be strongly dependent of the intensity of solar irradiance.

Keywords: Photodynamic effect; Senescent phytoplankton; Latitude; Polar regions; Solar irradiance.

48 **1. Introduction**

49 Reconstructions of sedimentary palaeoenvironments are essential to place the current global
50 warming trends into the context of natural and long-term climate variability. Lipid biomarkers
51 preserved in sediments are often used for this purpose since they are key indicators of organic
52 matter (OM) sources (Volkman et al., 1998; Wakeham et al., 1997). Maximizing the reliability
53 of these reconstructions requires careful consideration of the processes that affect the fate of
54 OM – notably OM degradation and/or preservation – during its transport down the water
55 column from the euphotic zone to the seafloor. Degradation may be biotic (i.e. induced by
56 zooplankton and bacteria, Harvey et al., 1987; Grossart et al., 2007) or abiotic (i.e. induced by
57 light or radicals, Rontani, 2012). Photooxidation (which has generally received little attention
58 until now in the literature) that destroys most of the unsaturated components of biogenic OM
59 initially present in the settling material (for a recent review see Rontani and Belt, 2020) can
60 strongly alter the lipid signature of OM reaching the seafloor. It is thus essential to take into
61 account the potential effects of abiotic degradation when making palaeoenvironmental
62 reconstructions from sedimentary OM.

63 In healthy phytoplankton cells, light absorption by chlorophyll creates an excited singlet
64 state (^1Chl), which leads to the classical fast reactions of photosynthesis (Foote, 1976). The
65 energy of this excited state is then transferred to various substrates, where it promotes
66 photosynthetic reactions, while a relatively small proportion of ^1Chl (<0.1%) undergoes
67 intersystem crossing (ISC) to form the longer-lived triplet state (^3Chl ; Knox and Dodge, 1985)
68 (Fig. 1). ^3Chl is not only potentially damaging in itself in Type I reactions (Knox and Dodge,
69 1985), but can also generate reactive singlet oxygen ($^1\text{O}_2$) by reaction with ground state oxygen
70 ($^3\text{O}_2$) via Type II photoprocesses (Fig. 1) (Krieger-Liszkay, 2005). Despite the production of
71 other Reactive Oxygen Species (ROS), it is generally considered that the photo-production of
72 $^1\text{O}_2$ plays the major role in light-induced damage to plant cells (Triantaphylides et al., 2008).

73 In view of the susceptibility of plant cells to oxidative damage, there are many antioxidant
74 protective mechanisms in chloroplasts. For example, carotenoids quench ^3Chl and $^1\text{O}_2$ by
75 energy transfer mechanisms at very high rates (Fig. 1). Such antioxidants have a dual role: first,
76 they limit $^1\text{O}_2$ formation, and second, they help remove any $^1\text{O}_2$ that does form (Foote, 1976;
77 Tefler, 2002). Tocopherols and ascorbic acid are also efficient quenchers of $^1\text{O}_2$ (Halliwell,
78 1987; Havaux et al., 2005).

79 In senescent phototrophic organisms, the cessation of photosynthetic reactions results in
80 an accelerated rate of formation of ^3Chl and ROS (mainly $^1\text{O}_2$) (Nelson, 1993; Triantaphylides
81 et al., 2008). The rate of formation of these potentially damaging species then often exceeds the
82 quenching capacity of the photoprotective system such that photodegradation of cell
83 components can occur via the so-called photodynamic effect (Merzlyak and Hendry, 1994)
84 (Fig. 1). Direct and irreversible reaction of ^3Chl with $^3\text{O}_2$ (photobleaching) gives photooxidation
85 products (Harbour and Bolton, 1978) (Fig. 1), while $^1\text{O}_2$ reacts extremely rapidly with nearby
86 biomolecules at near diffusion-controlled rates (photodynamic effect) (Knox and Dodge, 1985;
87 Cadenas, 1989; Skovsen et al., 2005). The very high reactivity of $^1\text{O}_2$ with numerous cell
88 components (unsaturated lipids, some amino acids, nucleic acids; Rontani, 2012, Devasagayam
89 and Kamat, 2002) is a consequence of the loss of the spin restriction that normally hinders
90 reaction of $^3\text{O}_2$ with these biomolecules (Zolla and Rinalducci, 2002). $^1\text{O}_2$ also reacts with the
91 sensitizer (chlorophyll) inducing its photobleaching (Nelson, 1993; Rontani, 2012) (Fig. 1). It
92 is important to note, however, that photobleaching of the sensitizer reduces $^1\text{O}_2$ production and
93 is thus competitive with the photodynamic effect.

94 In this study, we investigated the photooxidation of chlorophyll (photobleaching) and
95 some common algal unsaturated lipids (Δ^5 -sterols and monounsaturated fatty acids (MUFAs))
96 (photodynamic effect) in marine particulate matter from locations representing a diverse range
97 of latitudes, from the Arctic to the Antarctic. In order to try to explain an increased, yet highly

98 variable, efficiency of the photodynamic effect observed in material from the polar regions,
99 particular attention was given to samples from the Canadian Arctic representing sea ice, the
100 water column under the ice, and regions of open water.

101

102 **2. Experimental**

103

104 *2.1. Sample collection*

105 Detailed descriptions (e.g. sampling dates, depths, volumes, etc) of the collection of samples of
106 marine particulate matter from the Arctic, English Channel, Mediterranean Sea, Arabian Sea,
107 Equatorial Pacific, Equatorial Atlantic, Peru upwelling and East Antarctica (Fig. 2) has been
108 described previously (see references in Tables 1 and 2). Briefly, suspended particulate matter
109 (SPM) samples were collected with Niskin bottles or an in situ multiple-unit large-volume
110 filtration system (MULVFS), while sinking particles were collected with floating or fixed
111 mooring sediment traps. Sub-samples for lipid analysis were then filtered onto GF/F filters and
112 stored frozen ($-80\text{ }^{\circ}\text{C}$). Sympagic algae were obtained from the bottom-most layer of sea ice
113 (0-10 cm) from Resolute Passage (Canadian Arctic) (Rontani et al., 2014). Samples of the sub-
114 ice colonial diatom, *Melosira arctica*, which colonises the underside of sea ice and is widely
115 distributed across the Arctic (Boetius et al., 2013), were collected from the Canadian icebreaker
116 CCGS Amundsen under the ice ($49 \pm 4\text{ cm}$) in Baffin Bay ($70^{\circ}28'32''\text{N}$, $64^{\circ}0'37''\text{W}$) in June
117 2016 (GreenEdge Campaign)) and on board of R/V Lance ($81^{\circ}14'22''\text{N}$, $21^{\circ}54'50''\text{E}$) in
118 August 2017 as part of an oceanographic transect north of Svalbard from Rijpfjorden towards
119 the Nansen Basin. Near-surface ($<10\text{ m}$) water column samples (ca. 1 – 4 l) were collected
120 along a N-S transect terminating in the Amundsen Sea (Antarctica) and filtered (GF/F) on board
121 the Korean Icebreaker RV Araon in January/February 2016.

122

123 *2.2. Sample treatment*

124 The whole material of the different samples was reduced with excess NaBH₄ in MeOH (25 ml;
125 30 min) to reduce labile hydroperoxides (resulting from Type II photooxidation) to their
126 corresponding alcohols, which are more amenable to analysis using gas
127 chromatography/electron ionization mass spectrometry (GC-EIMS), gas
128 chromatography/electron ionization tandem mass spectrometry (GC-EIMS/MS) and gas
129 chromatography/electron ionization quadrupole time of flight mass spectrometry (GC-QTOF).
130 Water (25 ml) and KOH (2.8 g) were then added and the resulting mixture saponified by
131 refluxing (2 h). After cooling, the mixture was acidified (HCl, 2 N) to pH 1 and extracted with
132 dichloromethane (DCM; 3 x 20 ml). The combined DCM extracts were dried over anhydrous
133 Na₂SO₄, filtered and concentrated via rotary evaporation at 40 °C to give total lipid extracts
134 (TLEs). All the solvents (pesticide/glass distilled grade) and reagents (Puriss grade) were
135 obtained from Rathburn and Sigma-Aldrich, respectively. TLEs were derivatized by dissolving
136 them in 300 µL pyridine/bis-(trimethylsilyl)trifluoroacetamide (BSTFA; Supelco; 2:1, v/v) and
137 silylated (50 °C, 1 h). After evaporation to dryness under a stream of N₂, the derivatized residue
138 was dissolved in hexane/BSTFA (to avoid desilylation) and analysed by the aforementioned
139 mass spectrometric methods.

140

141 *2.3. Assignment and quantification of lipids and their degradation products*

142 Lipids and their degradation products were identified by comparison of retention times and
143 mass spectra with those of standards and quantified using GC-EIMS, GC-EIMS/MS and GC-
144 QTOF based on calibrations with external standards. Operating conditions employed during
145 these analyses were as per those described previously (Rontani et al, 2019 and references
146 therein). Standards of phytol, palmitoleic acid, 24-methylcholesta-5,22-dien-3β-ol
147 (brassicasterol) and 24-methylcholesta-5,(24/28)-dien-3β-ol (24-methylenecholesterol) were

148 obtained from Sigma-Aldrich. Standard oxidation products of these compounds were produced
149 according to previously described procedures (Rontani and Marchand 2000; Marchand and
150 Rontani 2001; Rontani and Aubert, 2005).

151

152 *2.4. Data treatment*

153

154 *2.4.1 Chlorophyll photooxidation estimates*

155 The molar ratio 3-methylidene-7,11,15-trimethylhexadecan-1,2-diol (phytyldiol):phytol
156 (Chlorophyll Phytyl side-chain Photodegradation Index, CPPI) has been previously proposed
157 to estimate the extent of photodegradation of chlorophylls possessing a phytyl side-chain in
158 natural marine samples through use of the empirical equation: chlorophyll photodegradation %
159 = $(1 - [\text{CPPI} + 1]^{-18.5}) \times 100$ (Cuny et al., 1999).

160

161 *2.4.1. Lipid photooxidation estimates*

162 The extent of photooxidation (%) of sterols was estimated using the equation: Δ^5 -sterol
163 photooxidation % = $(\Delta^4\text{-stera-}6\alpha/\beta\text{-diols \%} \times (1+0.3)/0.3)$ (Christodoulou et al., 2009).

164 Type II photosensitized oxidation of MUFAs was estimated after quantification of
165 isomeric *trans* allylic hydroxyacids resulting from NaBH₄-reduction of the corresponding
166 photochemically-produced hydroperoxides after subtraction of the amounts of these
167 compounds arising from autoxidation (Marchand and Rontani, 2001).

168

169 *2.4.3. Statistical analysis*

170 Mann – Whitney – Wilcoxon tests were performed to identify any significant differences in: (i)
171 the ratio of brassicasterol photo-oxidation percentage / chlorophyll photo-oxidation percentage
172 with latitude (Table S1), and (ii) the ratios of 24-methylenecholesterol photooxidation

173 percentage / chlorophyll photooxidation percentage, palmitoleic acid photooxidation
174 percentage / chlorophyll photooxidation percentage and brassicasterol photooxidation
175 percentage / chlorophyll photooxidation percentage between different sample types (i.e. sea ice
176 POM, SPM and sediment traps) (Table S2).

177 **3. Results and discussion**

178 Since photodynamic processes and sensitizer photobleaching are competitive processes (Fig.
179 1), we used the ratio of the % photooxidation of membrane lipids to that of chlorophyll to
180 estimate the efficiency of Type II photosensitized oxidation processes (the photodynamic effect
181 in Fig. 1) in senescent phytoplankton at different latitudes. In the case of brassicasterol, a
182 phytoplanktonic Δ^5 -sterol widely distributed in the oceans (Volkman, 1986, 2003), values of
183 this ratio obtained from previously published and unpublished data sets (Table 1) show a strong
184 increase (albeit with high variability) in samples from the polar regions in comparison to
185 samples collected from temperate and equatorial settings (Fig. 3). Such increases were found
186 to be significant when the data from the temperate and equatorial settings were compared with
187 those from the Arctic and Antarctic datasets (and the combined Arctic/Antarctic dataset), yet
188 no significant difference was found between the high latitude datasets (Table S1). Low
189 temperatures have previously been shown to reduce diffusion rate of $^1\text{O}_2$ through cell
190 membranes (Ehrenberg et al., 1998), thus favouring the intra-cellular involvement of the
191 photodynamic effect. More recently, Amiraux et al. (2016) confirmed these results in the case
192 of the centric diatom *Chaetoceros neogracilis* (strain RCC2022) and observed an increase (3.0
193 ± 0.5 fold) of the ratio $k_{\text{camp}}/k_{\text{chl}}$ (where k_{camp} is the first-order photodegradation rate of
194 campesterol and k_{chl} this of chlorophyll) when the temperature decreased from 17 to 7°C. The
195 characteristic low temperatures of the Arctic and Antarctic could thus be the cause of the high
196 values of the ratio % photooxidation brassicasterol / % photooxidation chlorophyll measured in

197 samples from these regions. However, low temperatures alone cannot explain the very high
198 variability of this ratio observed within these samples (Fig. 3).

199 In an effort to explain this strong variability, we examined, more closely, Arctic samples
200 collected from sea ice, under the ice (suspended and sinking particles) and from open water
201 conditions (sinking particles), which are all dominated by diatoms. The % photooxidation of
202 the common diatom lipids brassicasterol, 24-methylenecholesterol and palmitoleic acid to that
203 of chlorophyll are summarized in Table 2 and Fig. 4. Strong differences of photodynamic effect
204 efficiency were observed between these different kinds of particles. These differences were
205 found to be significant between surface samples (sea ice and SPM) and traps and between under
206 ice traps and open water traps (Table S2). These different samples having been collected at very
207 close temperatures (ranging from -1 to -2 °C in surface waters of Arctic), it is clear that the low
208 temperatures do not represent the main driver for the enhancement of photodynamic efficiency
209 in polar regions.

210 Riebesell et al. (1991) previously suggested that growing cells released by sea ice remain
211 largely unaggregated (i.e. mainly in suspension). The very low photooxidation state of lipids
212 and chlorophyll observed in SPM collected under the ice (Fig. 4) could thus result from the
213 healthy state of the algal cells present in these samples (Rontani et al., 2016), which are largely
214 unaffected by photooxidative damage. Indeed, in healthy cells, the greater part of the
215 photoexcited chlorophyll singlet state is used in the fast photochemical reactions of
216 photosynthesis.

217 The efficiency of the photodynamic effect appears to be considerably higher in material
218 collected in sediment traps in spring from under sea ice compared to those collected in summer
219 from open water (Fig. 4, Table S2), which is likely attributable to the respective contributions
220 of sympagic (i.e. living within ice) vs pelagic algae. Indeed, in contrast to healthy and largely
221 unaggregated sympagic algal cells (see above), less metabolically-active sea ice algae that are

222 released from the ice are generally concentrated into aggregates that become sinking particles
223 (Riebesell et al., 1991). Moreover, sympagic diatoms exhibit a higher sensitivity towards light-
224 induced stress than pelagic diatoms (Kvernvik et al., 2020). Such differences in sensitivity were
225 attributed, in part, to the gradually changing and low amplitude irradiance typically experienced
226 by sympagic algae (Hill et al., 2018), whereas pelagic cells in open water, in contrast,
227 experience high amplitude changes in light intensity over much shorter timescales (MacIntyre
228 et al., 2000). This interesting hypothesis is not supported, however, by: (i) the very low
229 efficiency of the photodynamic effect observed in the bottom-most layer of sea ice (Table 2)
230 and (ii) the lack of correlation between lipid photooxidation % and the concentration of the sea
231 ice lipid biomarker IP₂₅ (a well-known sea ice proxy, for reviews see Belt and Müller, 2013;
232 Belt, 2018) in under ice traps ($R^2 < 0.008$).

233 During in vitro experiments carried out on senescent cells of the centric diatom
234 *Chaetoceros neogracilis* (strain RCC2022), Type II photosensitized oxidation of lipids was also
235 observed to be strongly enhanced by low irradiance levels, whereas the opposite was true for
236 the photodegradation of chlorophyll (Amiriaux et al., 2016). The ratio k_{camp}/k_{chl} thus increased
237 4.2 ± 0.8 fold when irradiance decreased from 2038 to 165 $\mu\text{mol photons m}^{-2} \text{s}^{-1}$. In the Arctic,
238 the mean PAR (Photosynthetically Active Radiation) irradiance in the surface mixed layer is
239 considerably higher in open water than in ice-covered zones (365 ± 62 and 10.9 ± 2.7 μmol
240 $\text{photons m}^{-2} \text{s}^{-1}$, respectively, Alou-Font et al., 2016). The intensity of solar irradiance may thus
241 be at the origin of the contrasting efficiency of the photodynamic effect observed in sinking
242 particles collected under sea ice compared to those from open water (Fig. 4). Further, the
243 increase of this efficiency with depth in under ice samples (Fig.4, Table S2) could result from
244 enhanced aggregation of senescent sympagic algae as they sink to deeper traps (Riebesell et al.,
245 1991; Rontani et al., 2016) where light transmission is lower. In contrast, the relatively high
246 irradiance observed at the ice-water interface (up to ca. 100 $\mu\text{mol photons m}^{-2} \text{s}^{-1}$ in Davis

247 Strait, Galindo et al., 2017) could explain the greatly diminished photodynamic effect in
248 sympagic algae inhabiting the bottom-most layer of sea ice and in *Melosira arctica* (Table 2)
249 (Fig. 6). Examination of near-surface (<10 m) SPM samples collected along a N-S transect
250 terminating in the Amundsen Sea (Antarctica) in open water and seasonally ice covered zones
251 further confirmed the increase of photodynamic efficiency in regions of sea ice cover (Fig. 5)
252 ($W = 52$, $p\text{-value} = 0.003205$). In addition, the relatively higher photooxidation state of these
253 suspended particles compared to those collected in the Arctic (Fig. 4, Table 2) may be attributed
254 to the low contribution (typically 0.5 to 2%) of sympagic algae to primary production in
255 January-February in the Antarctic (Lizotte, 2001).

256 Due to their strong aggregation capability (Macdonald et al., 1998; Ambrose et al., 2001,
257 2005) and the low remineralizing potential of their associated bacteria (Amiriaux et al., 2017,
258 2020), sympagic algae seem to contribute more significantly than open water phytoplankton to
259 the export of carbon to Arctic sediments, providing an early season food source for benthic
260 fauna (Macdonald et al., 1998; Mincks et al., 2005). Episodic massive falls of *M. arctica* can
261 sink to the seafloor (Ambrose et al., 2005; Boetius et al., 2013; Lalande et al., 2019). The
262 polyunsaturated fatty acid (PUFA) content in algal biomass that reached the seafloor is essential
263 for growth and reproduction of benthic fauna (Brett and Müller-Navarra, 1997; McMahon et
264 al., 2006). Due to the high photosensitized oxidation of MUFAs observed in samples sinking
265 under sea ice cover (Fig. 4), and the well-known increasing photooxidation rates of fatty acids
266 with their degree of unsaturation (Frankel, 1998; Rontani et al., 1998), the PUFA content of
267 sympagic material reaching the sediment would thus be greatly reduced. *Melosira* strands that
268 are weakly affected by abiotic degradation processes under the ice (ratio C_{20:5} acid vs
269 palmitoleic acid ranging from 0.25 to 0.47), despite a significant photooxidation of chlorophyll
270 (Table 2), and that sink very quickly to the seafloor (Syvertsen, 1991) in massive falls (Ambrose

271 et al., 2005; Boetius et al., 2013; Lalande et al., 2019) may be an important source of fresh
272 material rich in OM (i.e., PUFAs) for the benthos.

273 Further, the expected reduction of sea ice cover resulting from increased global warming
274 may result in a shift in the relative contributions of ice-associated vs pelagic algae (Carroll and
275 Carroll, 2003) to the seafloor. The high flux of fast-sinking aggregates of strongly abiotically-
276 altered sympagic algae and fast sinking well preserved *M. arctica* reaching Arctic sediments
277 could thus be replaced, progressively, by a lower flux of weakly abiotically altered pelagic
278 biomass. Such a shift should thus strongly impact the quality and quantity of food reaching
279 benthic communities, as previously proposed by Sun et al. (2007), and could significantly alter
280 the community structure and spatial distribution of the benthos.

281

282 **4. Conclusions**

283 During this work, Type II photosensitized oxidation of lipids (photodynamic effect) and
284 photodegradation of chlorophyll (photobleaching) were compared in several samples of
285 particulate matter from locations ranging from the Arctic to the Antarctic. The results obtained
286 clearly showed an enhancement of the photooxidation of lipids at the expense of chlorophyll
287 photodegradation in polar regions compared to temperate and equatorial regions. Careful
288 examination of different samples of sympagic and epiphytic algae, suspended and sinking
289 particles collected in Arctic allowed to show that the efficiency of photodynamic effect was
290 particularly high in sinking particles collected under the ice (Fig. 6). This high efficiency was
291 attributed to the rapid settling of highly aggregated sympagic algae to depths of low light
292 transmission favouring photodynamic effect at the expense of photobleaching of the sensitizer.
293 In contrast, in the case of samples exposed to relatively high solar irradiances - sympagic and
294 epiphytic algae collected in the bottommost layer of ice or at the underside of ice, respectively,
295 and particles collected from open waters - the efficiency of photodynamic effect appeared to be

296 relatively weak (Fig. 6). The low efficiency of Type II photosensitized oxidation of lipids
297 observed in temperate and equatorial regions could, perhaps paradoxically, thus be attributed
298 to the high solar irradiances received in these regions. The intensity of solar irradiance seems
299 thus to be a key parameter during the Type II photosensitized oxidation of lipids in senescent
300 phytoplankton.

301

302 **Acknowledgements**

303 The sediment trap samples off Peru were collected thanks to the AMOP (“Activity of research
304 dedicated to the Minimum of Oxygen in the eastern Pacific”) project. We would like to thank
305 the crews of the German R/V Meteor, Peruvian R/V Olaya and French R/V Atalante for the
306 AMOP fixed mooring servicing. We would like to thank M. Soto (IRD, Peru), E. Carrasco
307 (IMARPE, Peru) and J. Grelet (IMAGO/IRD, France), as well as O. De Gesincourt, L.
308 Scouarnec, A. Royer and E. De Saint Léger (DT-INSU/CNRS, France) for general logistics and
309 administrative support. We would like also to thank C. Panagiotopoulos (MIO, France) and
310 F.O. Velazco (IMARPE, Peru) for the sediment trap sampling, N. Leblond (OOV, France) and
311 M. Bretagnon (LEGOS) for the initial samples processing, as well as A. Oschlies for a
312 complementary SFB754 funding. Equatorial Pacific and Arabian Sea samples were collected
313 under the auspices of the U.S. Joint Global Ocean Flux Program through U.S. National Science
314 Foundation grants OCE-90-22319 and OCE-9310364, respectively, to SGW. Sediment trap
315 samples from the Beaufort Sea were obtained through the Long-Term Oceanic Observatories
316 Program of the ArcticNet Network of Centres of Excellence (NCE) of Canada. Thanks are due
317 to the scientific party and crew of cruise NBP1402 funded by NSF (ANT-1143836) for the
318 sampling of Antarctic samples. Collection of Resolute Passage samples (sea ice, SPM and
319 sinking particles) was supported through a University of Manitoba Start-up grant and Natural
320 Sciences and Engineering Research Council of Canada (NSERC). We thank the Captain and

321 crew of the R.V ‘Tethys II’ (Institut National des Sciences de l’Univers, France) for assistance
322 in the field during recovery and deployment of the trap mooring in Ligurian Sea. We
323 acknowledge GBMF-MMI Grants 2293 and 2928 and NSF-OCE-0934095 for the financial
324 support provided to Amazon plume collections, as well as the Brazilian government (Ministério
325 da Marinha). Thanks are due to Philipp Assmy for collecting a sample of *Melosira arctica*
326 during the Rijpfjorden transect which was funded by the former Centre for Ice, Climate and
327 Ecosystems at the Norwegian Polar Institute. Thanks are also due to the scientific party and
328 crew of cruise NBP1402 funded by NSF (ANT-1143836) for the sampling of East Antarctic
329 samples. Samples from the Amundsen Sea transect were collected as part of the project
330 ‘Variability of carbon pump and climate control in the Southern Ocean’ (PE20140). Further,
331 we thank the FEDER 1166-39417 for the funding of the apparatus employed. We are also
332 grateful to two anonymous reviewers for their useful and constructive comments.

333

334 References

- 335 Alou-Font, E., Roy, S., Agusti, S., Gosselin, M., 2016. Cell viability, pigments and
336 photosynthetic performance of Arctic phytoplankton in contrasting ice-covered and open-
337 water conditions during the spring–summer transition. *Mar. Ecol. Prog. Ser.* 543, 89-106.
- 338 Ambrose, W.G., Clough, L.M., Tilney, P.R., Beer, L., 2001. Role of echinoderms in benthic
339 remineralization in the Chukchi Sea. *Mar. Biol.* 139, 937–949.
- 340 Ambrose, W.G., Quillfeldt, Jr.C., Clough, L.M., Tilney, P.V.R., Tucker, T., 2005. The sub-ice
341 algal community in the Chukchi Sea: large- and small-scale patterns of abundance based
342 on images from a remotely operated vehicle. *Polar Biol.* 28, 784-795.
343 doi:10.1007/s00300-005-0002-8

344 Amiraux, R., Jeanthon, C., Vaultier, F., Rontani, J.-F., 2016. Paradoxical effects of temperature
345 and solaire irradiance on the photodegradation state of killed phytoplankton. *J. Phycol.*
346 52, 475-485.

347 Amiraux, R., Belt, S.T., Vaultier, F., Galindo, V., Gosselin, M., Bonin, P., Rontani, J.-F., 2017.
348 Monitoring photo-oxidative and salinity-induced bacterial stress in the Canadian Arctic
349 using specific lipid tracers. *Mar. Chem.* 194, 89–99.
350 doi.org/10.1016/j.marchem.2017.05.006.

351 Amiraux R., Burot C., Bonin P., Massé, G., Guasco, S., Babin, M., Vaultier, F., Rontani, J.-F.,
352 2020. Stress factors resulting from the Arctic vernal sea ice melt: impact on the viability
353 of the bacterial communities associated to sympagic algae. *Elem. Sci. Anth.* (In press).

354 Belt, S.T., Müller, J., 2013. The Arctic sea ice biomarker IP₂₅: a review of current
355 understanding, recommendations for future research and applications in palaeo sea ice
356 reconstructions. *Quarter. Sci. Rev.* 79, 9–25. doi.10.1016/j.quascirev.2012.12.001

357 Belt, S.T., 2018. Source-specific biomarkers as proxies for Arctic and Antarctic sea ice. *Org.*
358 *Geochem.* 125, 273-295.

359 Boetius, A., Albrecht, S., Bakker, K., Bienhold, C., Felden, J., Fernandez-Méndez, M.,
360 Hendricks, S., Kathein, C., Lalande, C., Krumpen, T., Nicolaus, M., Peeken, I., Rabe, B.,
361 Rogacheva, A., Rybakova, E., Somavilla, R., Wenzhöfer, F., RV Polarstern ARK27-3-
362 shipboard Science Party., 2013. Export of algal biomass from the melting Arctic sea ice.
363 *Science* 339, 1430–1432. doi.10.1126/science.1231346

364 Bretagnon, M., Paulmier, A., Garçon, V., Dewitte, B., Illig, S., Leblond, N., Coppola, L.,
365 Campos, F., Velazco, F., Panagiotopoulos, C., Oschlies, A., Hernandez-Ayon, J.M.,
366 Vergara, O., Montes, I., Martinez, P., Carrasco, E., Grelet, J., Depretz de Gesincourt, O.,
367 Maes, C., Scouarnec, L. Modulation of the vertical particle transfer efficiency in the

368 Oxygen Minimum Zone off Peru., 2018. *Biogeoscience* 15, 5093-5111.
369 doi.org/10.5194/bg-15-5093-2018

370 Brett, M.T., Müller-Navarra, D.C., 1997. The role of highly unsaturated fatty acids in aquatic
371 food web processes. *Freshwater Biol.* 38, 483–499.

372 Cadenas, E., 1989. Biochemistry of oxygen toxicity. *Annu. Rev. Biochem.* 58, 79-110.

373 Carroll, M.L., Carroll, J., 2003. The Arctic seas. In: Black, K.D., Shimmield, G.B. (eds)
374 *Biogeochemistry of Marine Systems*. Blackwell, Oxford, pp 127–156.

375 Christodoulou, S., Marty, J.-C., Miquel, J.-C., Volkman, J.K., Rontani, J.-F., 2009. Use of lipids
376 and their degradation products as biomarkers for carbon cycling in the northwestern
377 Mediterranean Sea. *Mar. Chem.* 113, 25–40. doi.10.1016/j.marchem.2008.11.003

378 Cuny, P., Romano, J.-C., Beker, B., Rontani, J.-F., 1999. Comparison of the photodegradation
379 rates of chlorophyll chlorin ring and phytol side chain in phytodetritus: is the phytyldiol
380 versus phytol ratio (CPPI) a new biogeochemical index? *J. Exp. Mar. Biol. Ecol.* 237,
381 271–290. doi.10.1016/S0022-0981(99)00010-6

382 Devasagayam, T., Kamat, J., 2002. Biological significance of singlet oxygen. *Ind. J. Exp. Biol.*
383 40, 680–692.

384 Ehrenberg, B., Anderson, J.L., Foote, C.S., 1998. Kinetics and yield of singlet oxygen
385 photosensitized by hypericin in organic and biological media. *Photochem. Photobiol.* 68,
386 135–140. doi.10.1111/j.1751-1097.1998.tb02479.x

387 Foote, C.S., 1976. Photosensitized oxidation and singlet oxygen: consequences in biological
388 systems. In: Pryor, W.A. (Ed.), *Free Radicals in Biology*. Academic Press, New York,
389 pp. 85-133.

390 Frankel, E.N., 1998. *Lipid oxidation*. The Oily Press, Dundee.

391 Galeron, M.-A., Radakovitch, O., Charriere, B., Vaultier, F., Volkman, J.K., Bianchi, T.S.,
392 Ward, N.T., Medeiros, P., Sawakuchi, H., Tank, S., Kerhervé, P., Rontani J.-F., 2018.

393 Lipoxygenase-induced autoxidative degradation of terrestrial particulate organic matter
394 in estuaries: a widespread process enhanced at high and low latitudes. *Org. Geochem.*
395 115, 78-92.

396 Galindo, V., Gosselin, M., Lavaud, J., Mundy, C.J., Else, B., Ehn, J., Babin, M., Rysgaard, S.,
397 2017. Pigment composition and photoprotection of Arctic sea ice algae during spring.
398 *Mar. Ecol. Progr. Ser.* 585: 49–69. doi.org/10.3354/meps12398

399 Grossart, H.-P., Tang, K.W., Kjørboe, T., Ploug, H., 2007. Comparison of cell-specific activity
400 between free-living and attached bacteria using isolates and natural assemblages. *FEMS*
401 *Microbiol. Let.* 266, 194–200. doi.org/10.1111/j.1574-6968.2006.00520.x

402 Halliwell, B., 1987. Oxidative damage, lipid peroxidation and antioxidant protection in
403 chloroplasts. *Chem. Phys. Lipids* 44, 327-340.

404 Harbour, J. R., Bolton, J. R., 1978. The involvement of the hydroxyl radical in the destructive
405 photooxidation of chlorophylls in vivo and in vitro. *Photochem. Photobiol.* 28, 231-234.

406 Harvey, H.R., Eglinton, G., O'hara, S.C.M., Corner, E.D.S., 1987. Biotransformation and
407 assimilation of dietary lipids by *Calanus* feeding on a dinoflagellate. *Geochim.*
408 *Cosmochim. Acta* 51, 3031–3040. doi.org/10.1016/0016-7037(87)90376-0

409 Havaux, M., Eymery, F., Porfirova, S., Rey, P., Dormann, P., 2005. Vitamin E protects against
410 photoinhibition and photooxidative stress in *Arabidopsis thaliana*. *Plant Cell* 17, 3451-
411 3469.

412 Hill, V.J., Light, B., Steele, M., Zimmerman, R.C., 2018. Light availability and phytoplankton
413 growth beneath Arctic sea ice: integrating observations and modelling. *J. Geophys. Res.*
414 *Oceans* 123, 3651–3667. doi.org/10.1029/2017JC013617

415 Korytowski, W., Bachowski, G.J., Girotti, A.W., 1992. Photoperoxidation of cholesterol in
416 homogeneous solution, isolated membranes, and cells: comparison of the 5 α - and 6 β -

417 hydroperoxides as indicators of singlet oxygen intermediacy. *Photochem. Photobiol.* 56,
418 1-8.

419 Knox, J.P., Dodge, A.D., 1985. Singlet oxygen and plants. *Phytochemistry* 24, 889-896.

420 Krieger-Liszkay, A., 2005. Singlet oxygen production in photosynthesis. *J. Exp. Bot.* 56, 337–
421 346.

422 Kvernvik, A.C., Rokitta, S.D., Leu, E., Harms, L., Gabrielsen, T.M., Rost, B., Hoppe, C.J.M.,
423 2018. Higher sensitivity towards light stress and ocean acidification in an Arctic sea-ice-
424 associated diatom compared to a pelagic diatom. *New Phytol.* 226, 1708–1724. doi:
425 10.1111/nph.16501

426 Lalande, C., Nöthig, E.-M., Fortier, L., 2019. Algal export in the Arctic Ocean in times of global
427 warming. *Geophys. Res. Lett.* 46, 5959–5967. doi.org/10.1029/2019GL083167

428 Lizotte, M., 2001. The contributions of sea ice algae to Antarctic marine primary production.
429 *Amer. Zool.* 1, 57-73.

430 MacDonald, R.W., Solomon, S.M., Cranston, R.E., Welch, H.E., Yunker, M.B., Gobeil, C.,
431 1998. A sediment and organic carbon budget for the Canadian Mackenzie shelf. *Mar.*
432 *Geol.* 144, 255-273.

433 MacIntyre, H.L., Kana, T.M., Geider, R.J., 2000. The effect of water motion on short-term rates
434 of photosynthesis by marine phytoplankton. *Trends Plant Sci.* 5, 12-17.

435 MacMahon, K.W., Ambrose Jr, W.G., Johnson, B.J., Sun, M.Y., Lopez, G.R., Clough, L.M.,
436 Carroll, M.L., 2006. Benthic community response to ice algae and phytoplankton in Ny
437 Ålesund, Svalbard. *Mar. Ecol. Progr. Ser.* 310, 1-14.

438 Marchand, D., Rontani, J.-F., 2001. Characterisation of photo-oxidation and autoxidation
439 products of phytoplanktonic monounsaturated fatty acids in marine particulate matter and
440 recent sediments. *Org. Geochem.* 32, 287–304. doi.10.1016/S0146-6380(00)00175-3

441 Merzlyak, M.N., Hendry, G.A.F., 1994. Free radical metabolism, pigment degradation and lipid
442 peroxidation in leaves during senescence. *Proc. Roy. Soc. Edinburgh* 102B, 459-471.

443 Mincks, S.L., Smith, C.R., DeMaster, D.J., 2005. Persistence of labile organic matter and
444 microbial biomass in Antarctic shelf sediments: Evidence of a sediment food bank. *Mar.*
445 *Ecol. Progr. Ser.* 300, 3–19. doi.org/10.3354/meps300003.

446 Nelson, J.R., 1993. Rates and possible mechanism of light-dependent degradation of pigments
447 in detritus derived from phytoplankton. *J. Mar. Res.* 51, 155–179.
448 doi.10.1357/0022240933223837

449 Riebesell U., Schloss I., Smetacek V., 1991. Aggregation of algae released from melting sea
450 ice -implications for seeding and sedimentation. *Pol. Biol.* 11:239–248

451 Rontani, J.-F., Grossi, V., Faure, F., Aubert, C., 1994. “Bound” 3-methylidene-
452 7,11,15-trimethylhexadecan-1,2-diol: a new isoprenoid marker for the photodegradation
453 of chlorophyll-a in seawater. *Org. Geochem.* 21, 135–142. doi.org/10.1016/0146-
454 6380(94)90150-3

455 Rontani, J.-F., Cuny, P., Grossi, V., 1998. Identification of a pool of lipid photoproducts in
456 senescent phytoplanktonic cells. *Org. Geochem.* 29, 1215–1225. doi.org/10.1016/S0146-
457 6380(98)00073-4

458 Rontani, J.-F., Marchand, D., 2000. Δ^5 -Stenol photoproducts of phytoplanktonic origin: a
459 potential source of hydroperoxides in marine sediments? *Org. Geochem.* 31, 169-180.

460 Rontani, J.-F., Aubert, C., 2005. Characterization of isomeric allylic diols resulting from
461 chlorophyll phytyl side chain photo- and autoxidation by electron ionization gas
462 chromatography/mass spectrometry. *Rapid Commun. Mass Spectrom.* 19, 637-646.

463 Rontani, J.-F., Zabeti, N., Wakeham, S.G., 2011. Degradation of particulate organic matter in
464 the equatorial Pacific Ocean: biotic or abiotic? *Limnol. Oceanogr.* 56, 333-349.

465 Rontani, J.-F., 2012. Photo- and free radical-mediated oxidation of lipid components during the
466 senescence of phototrophic organisms. In: T. Nagata Ed., *Senescence*. Intech, Rijeka, pp.
467 3-31.

468 Rontani, J.-F., Charriere, B., Forest, A., Heussner, S., Vaultier, F., Petit, M., Delsaut, N.,
469 Fortier, L., Sempéré, R., 2012. Intense photooxidative degradation of planktonic and
470 bacterial lipids in sinking particles collected with sediment traps across the Canadian
471 Beaufort Shelf (Arctic Ocean). *Biogeosciences* 9, 4787–4802. doi.org/10.5194/bg-9-
472 4787-2012

473 Rontani, J.-F., Belt, S.T., Brown, T., Vaultier, F., Mundy, C.J., 2014. Identification of
474 sequential photo- and autoxidation of diatom lipids in Arctic sea ice. *Org. Geochem.* 77,
475 59-71.

476 Rontani, J.-F., Belt, S.T., Brown, T.A., Amiroux, R., Gosselin, M., Vaultier, F., Mundy, C.J.,
477 2016. Monitoring abiotic degradation in sinking versus suspended Arctic sea ice algae
478 during a spring ice melt using specific lipid oxidation tracers. *Org. Geochem.* 98, 82–97.
479 doi.org/10.1016/j.orggeochem.2016.05.016

480 Rontani, J.-F., Smik, L., Belt, S.T., Vaultier, F., Armbrecht, L., Leventer, A., Armand L.K.,
481 2019. Abiotic degradation of highly branched isoprenoid alkenes and other lipids in the
482 water column off East Antarctica. *Mar. Chem.* 210, 34-47.

483 Rontani, J.-F., Belt, S.T., 2020. Photo- and autoxidation of unsaturated algal lipids in the marine
484 environment: An overview of processes, their potential tracers, and limitations. *Org.*
485 *Geochem.* 139, 103941. doi.org/10.1016/j.orggeochem.2019.103941

486 Rontani, J.-F., Smik, L., Vaultier, F., Widdicombe, C., Belt S.T., 2021. Seasonal monitoring of
487 biotic and abiotic degradation of suspended particulate lipids in the western English
488 Channel suggests a link between bacterial 10S-DOX activity and production of free fatty
489 acids by wounded diatoms. *Mar. Chem.* (In Press)

490 Skovsen, E., Snyder, J.W., Lambert, J.D.C., Ogilby, P.R., 2005. Lifetime and diffusion of
491 singlet oxygen in a cell. *J. Phys. Chem. B* 109, 8570–8573.

492 Sun, M.-Y., Carroll, M.L., Ambrose, W.G.Jr., Clough, L.M., Zou, L., Lopez, G.R., 2007. Rapid
493 consumption of phytoplankton and ice algae by Arctic soft-sediment benthic
494 communities: Evidence using natural and ¹³C-labeled food materials. *J. Mar. Res.* 65,
495 571-588.

496 Syvertsen, E.E., 1991. Ice algae in the Barents Sea: types of assemblages, origin, fate and role
497 in the ice edge phytoplankton bloom. *Polar Res.* 10, 277-287. doi:10.1111/j.1751-
498 8369.1991.tb00653.x

499 Telfer, A., 2002. What is beta-carotene doing in the photosystem II reaction centre? *Philos.*
500 *Trans. Roy. Soc. Lond. B Biol. Sci.* 357, 1431-1439.

501 Triantaphylides, C., Krischke, M., Hoerberichts, F.A., Ksas, B., Gresser, G., Havaux, M., Van
502 Breusegem, F., Johannes Mueller, M., 2008. Singlet oxygen is the major reactive Oxygen
503 species involved in photooxidative damage to plants. *Plant Physiol.* 148, 960-968.
504 doi/10.1104/pp.108.125690

505 Volkman, J.K. 1986. A review of sterol markers for marine and terrigenous organic matter.
506 *Org. Geochem.* 9, 83-99.

507 Volkman, J.K., Barrett, S.M., Blackburn, S.I., Mansour, M.P., Sikes, E.L., Gelin, F., 1998.
508 Microalgal biomarkers: a review of recent research developments. *Org. Geochem.* 29,
509 1163–1179.

510 Volkman, J.K. 2003. Sterols in microorganisms. *Appl. Microbiol. Biotechnol.* 60, 495-506.

511 Wakeham, S.G., Lee, C., Hedges, J.I., Hernes, P.J., Peterson, M.L., 1997. Molecular indicators
512 of diagenetic status in marine organic matter. *Geochim. Cosmochim. Acta* 61, 5363–
513 5369.

514 Wakeham, S.G., Peterson, M.L., Hedges J.I., Lee, C., 2002. Lipid biomarker fluxes in the
515 Arabian Sea: with a comparison to the Equatorial Pacific Ocean, *Deep-Sea Res.* 49, 2265-
516 2301.

517 Zolla, L., Rinalducci, S., 2002. Involvement of active oxygen species in degradation of light-
518 harvesting proteins under light stresses. *Biochem.* 41, 14391–14402.

519

Figure captions

520

521

522 **Figure 1.** Potential pathways for chlorophyll (Chl) excitation energy in senescent
523 phytoplankton cells (simplified scheme limited to the formation of $^1\text{O}_2$ and photoprotective role
524 of carotenoids (Car)).

525

526 **Figure 2.** Sampling locations.

527

528 **Figure 3.** Values of the ratio brassicasterol photooxidation %/chlorophyll photooxidation % in
529 particulate matter samples collected at different latitudes.

530

531 **Figure 4.** Values of the ratios brassicasterol photooxidation %/chlorophyll photooxidation %,
532 24-methylenecholesterol photooxidation %/chlorophyll photooxidation % and palmitoleic acid
533 photooxidation %/chlorophyll photooxidation % in particulate matter samples collected in
534 Arctic ice-covered and open water zones.

535

536 **Figure 5.** Values of the ratio brassicasterol photooxidation %/chlorophyll photooxidation % in
537 SPM samples collected in open and ice-covered zones along a N-S transect terminating in the
538 Amundsen Sea (Antarctica).

539

540 **Figure 6.** Conceptual scheme summarizing the efficiency of photodynamic effect in sympagic,
541 epiphytic and pelagic algae in polar regions. (To simplify the scheme only the Type II
542 photosensitized oxidation of palmitoleic acid is shown) (nd = not detected).

543

544 **Table captions**

545

546 **Table 1.** Variation of the ratio brassicasterol photooxidation %/chlorophyll photooxidation %
547 in particulate matter samples according to the latitude.

548

549 **Table 2.** Photooxidation of chlorophyll, brassicasterol, 24-methylenecholesterol and
550 palmitoleic acid in different sea ice, *M. arctica* and particulate matter samples collected in the
551 Arctic.

552

553 **Supplementary material**

554

555 **Table S1.** Results of Mann – Whitney – Wilcoxon analysis testing the effect of the latitude on
556 the brassicasterol photooxidation percentage : chlorophyll a photooxidation percentage ratio.
557 Bold values are indicative of significance.

558

559 **Table S2.** Results of Mann – Whitney – Wilcoxon analysis testing the effect of the sample type
560 on the 24-methylenecholesterol photo-oxidation percentage / chlorophyll photo-oxidation
561 percentage, palmitoleic acid photo-oxidation percentage / chlorophyll photo-oxidation
562 percentage and brassicasterol photo-oxidation percentage / chlorophyll photo-oxidation
563 percentage ratios. Bold values are indicative of significance.

Table 1

Variation of the ratio brassicasterol photooxidation %/chlorophyll photooxidation % in particulate matter samples according to the latitude.

Latitude	Location	Nature of particles	n	Brassicasterol hv %/Chlorophyll hv %	References
71-74°N	Canadian Arctic	Suspended and sinking	46	0.77 ± 1.10	Rontani et al., 2012; 2016
50°N	English Channel	Suspended	24	0.02 ± 0.04	Rontani et al., 2021
43°N	Rhône Prodelta	Suspended	21	0.21 ± 0.11	Galeron et al., 2018
43°N	Ligurian Sea	Sinking	12	0.21 ± 0.10	Christodoulou et al., 2009
17°N	Arabian Sea	Suspended and sinking	7	0.07 ± 0.04	Wakeham et al., 2002
0°	Equatorial Atlantic	Suspended	2	0.10 ± 0.12	Galeron et al., 2018
0°	Equatorial Pacific	Suspended and sinking	11	0.11 ± 0.07	Wakeham et al., 2002; Rontani et al., 2011
12°S	Peru Upwelling	Sinking	10	0.18 ± 0.04	Bretagnon et al., 2018
40-67°S	South Pacific	Suspended	5	0.09 ± 0.04	
67-75°S	Antarctica	Suspended	23	0.50 ± 0.45	Rontani et al., 2019

Table 2

Photooxidation of chlorophyll, brassicasterol, 24-methylenecholesterol and palmitoleic acid in different sea ice, *M. arctica* and particulate matter samples collected in the Arctic.

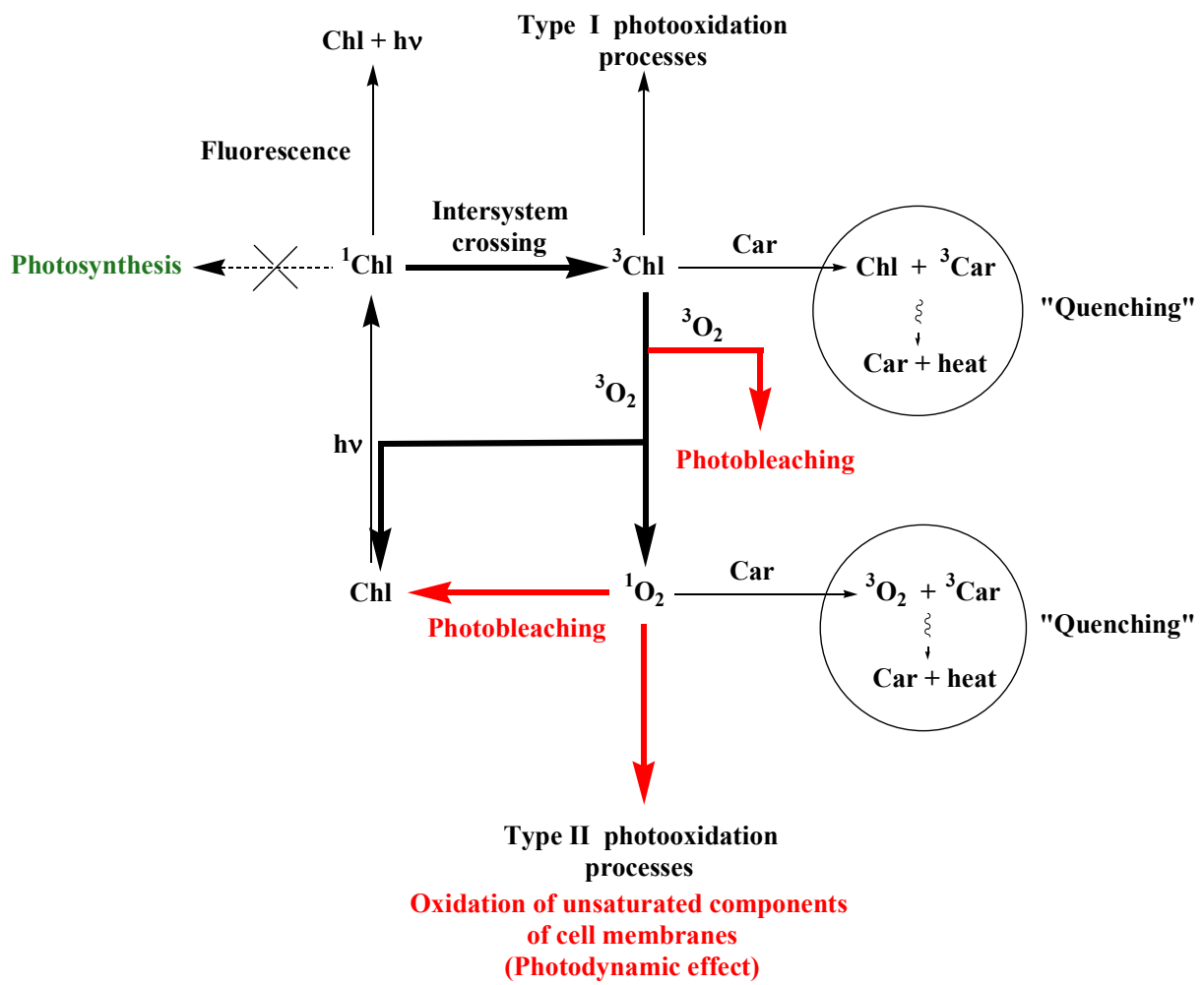
Samples	Location	n	Chlorophyll photooxidation %	Brassicasterol photooxidation %/ chlorophyll photooxidation %	24-Methylenecholesterol photooxidation %/ chlorophyll photooxidation %	Palmitoleic acid photooxidation %/ chlorophyll photooxidation %
Sea ice (0-3 cm)	Resolute Passage ^a and Davies Strait ^b	21	54.5 ± 38.4	0.02 ± 0.05	0.04 ± 0.10	0.05 ± 0.08
<i>Melosira arctica</i>	Baffin Bay and North of Svalbard	6	40.2 ± 12.8	-	-	0.03 ± 0.03
Under ice spm (<10 m)	Resolute Passage ^c	20	16.3 ± 13.9	0.05 ± 0.17	0.42 ± 0.96	1.00 ± 1.60
Under ice trap (5 m)	Resolute Passage ^c	11	55.7 ± 34.1	1.10 ± 0.62	1.22 ± 0.98	2.87 ± 2.78
Under ice trap (30 m)	Resolute Passage ^c	11	11.5 ± 8.6	2.00 ± 1.39	3.97 ± 2.22	8.39 ± 7.15
Open water trap (100 m)	Beaufort Sea ^d	12	99.8 ± 0.2	0.23 ± 0.07	0.48 ± 0.14	0.47 ± 0.19

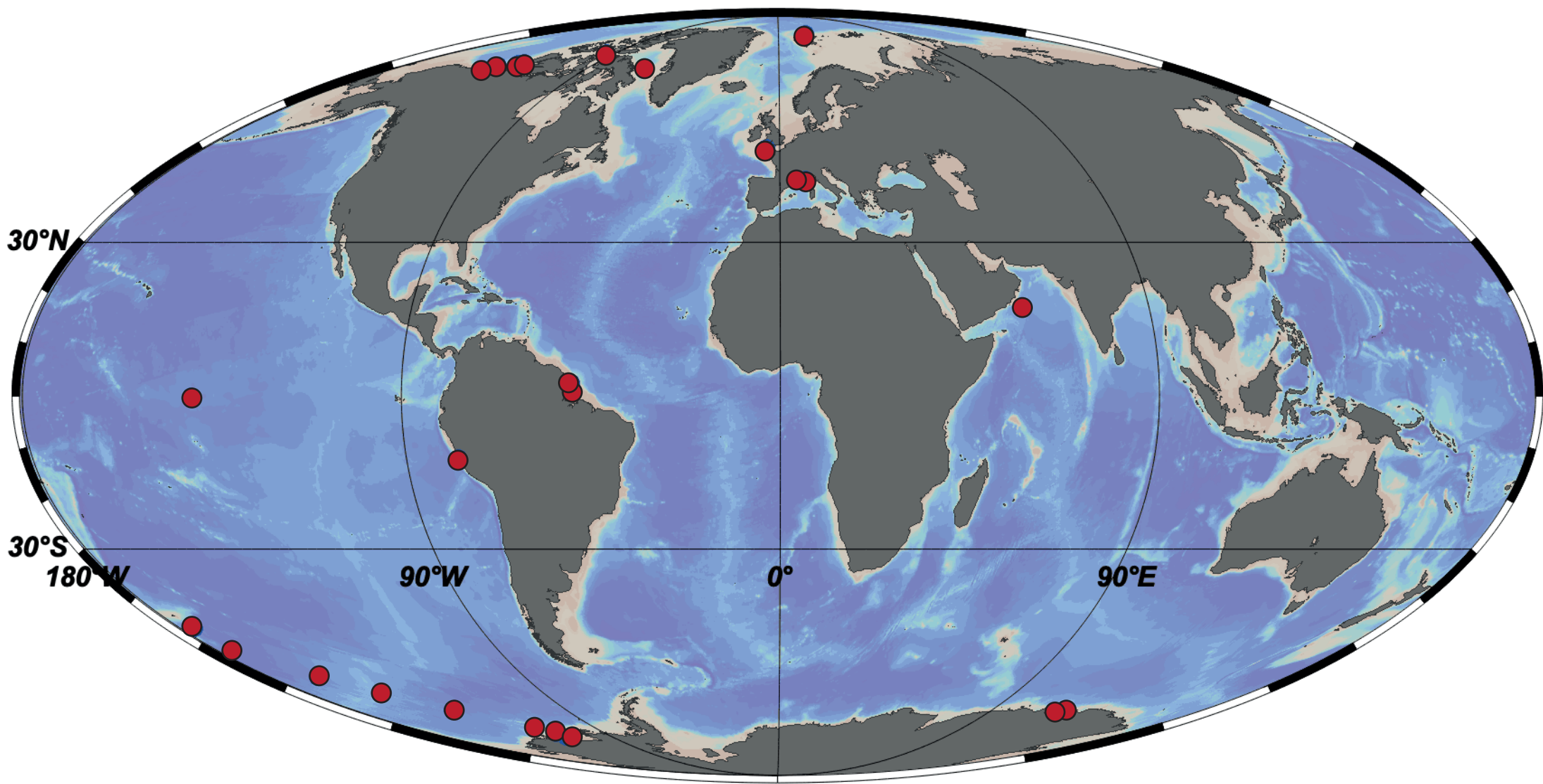
^a Rontani et al., 2014

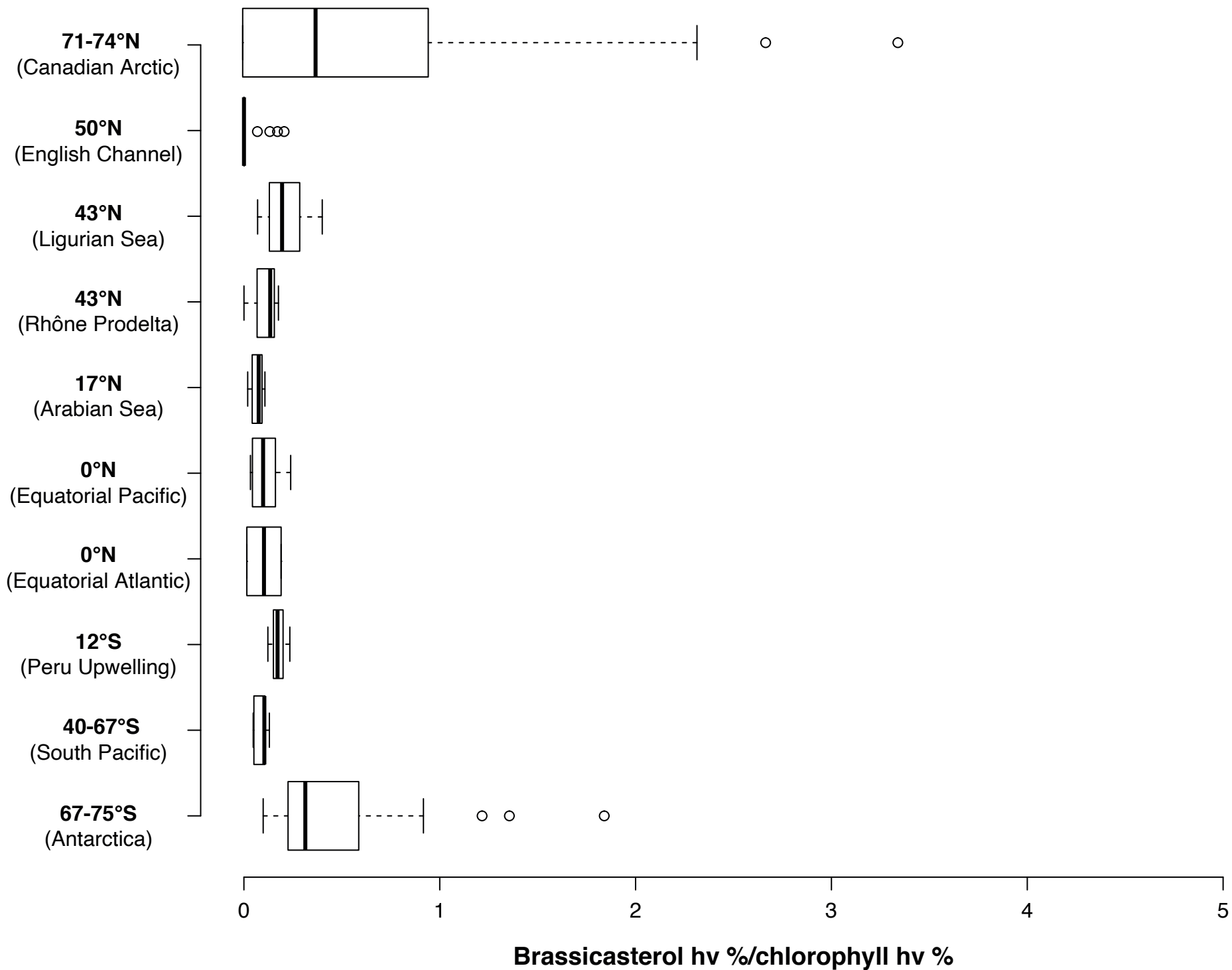
^b Amiraux et al., 2017

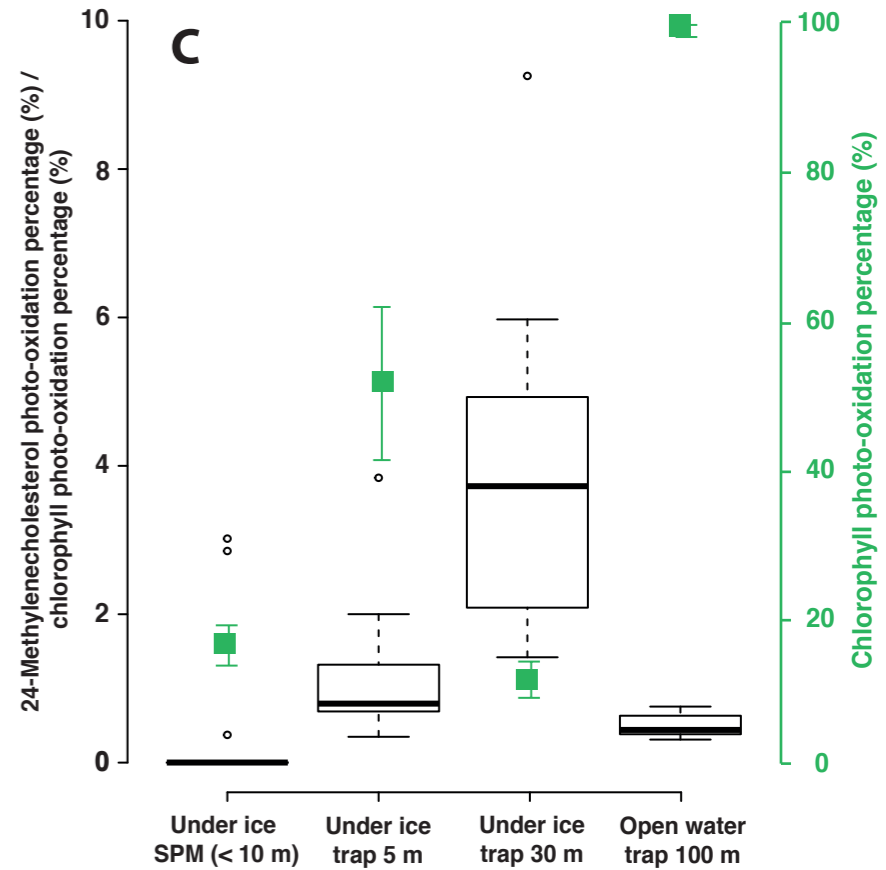
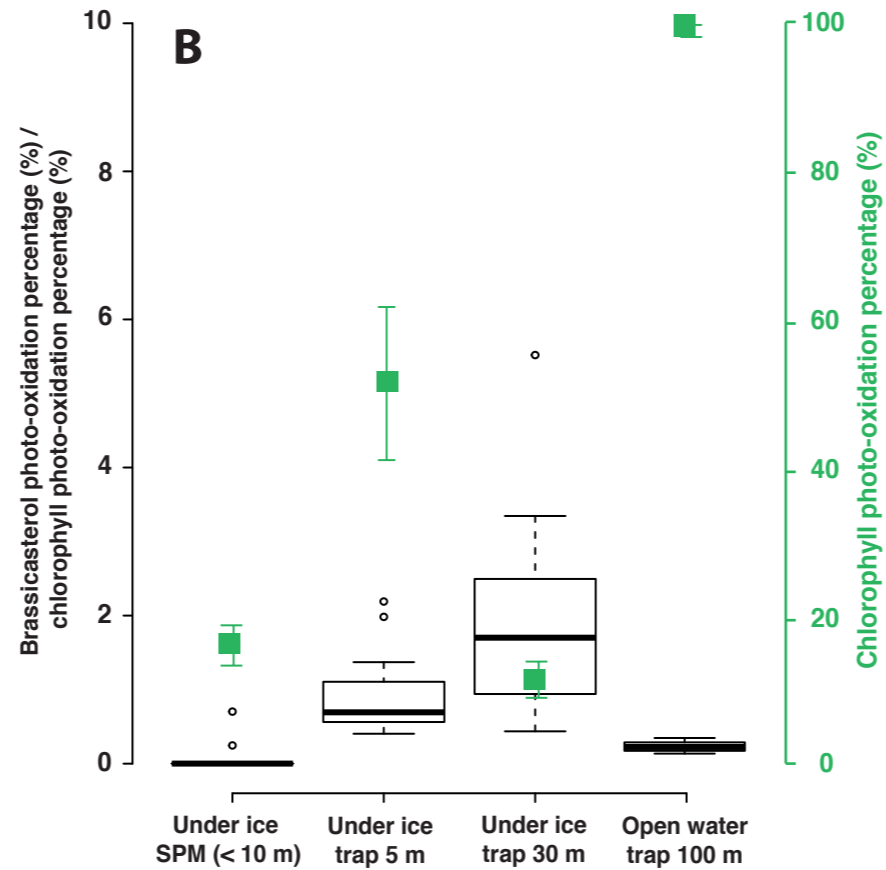
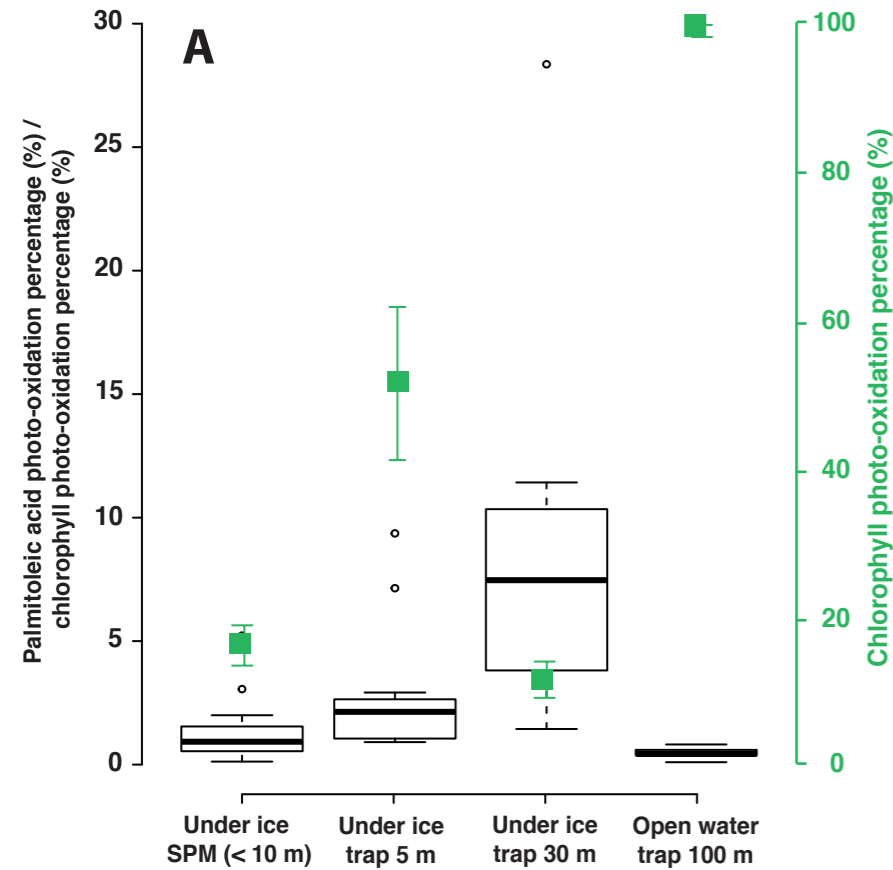
^c Rontani et al., 2016

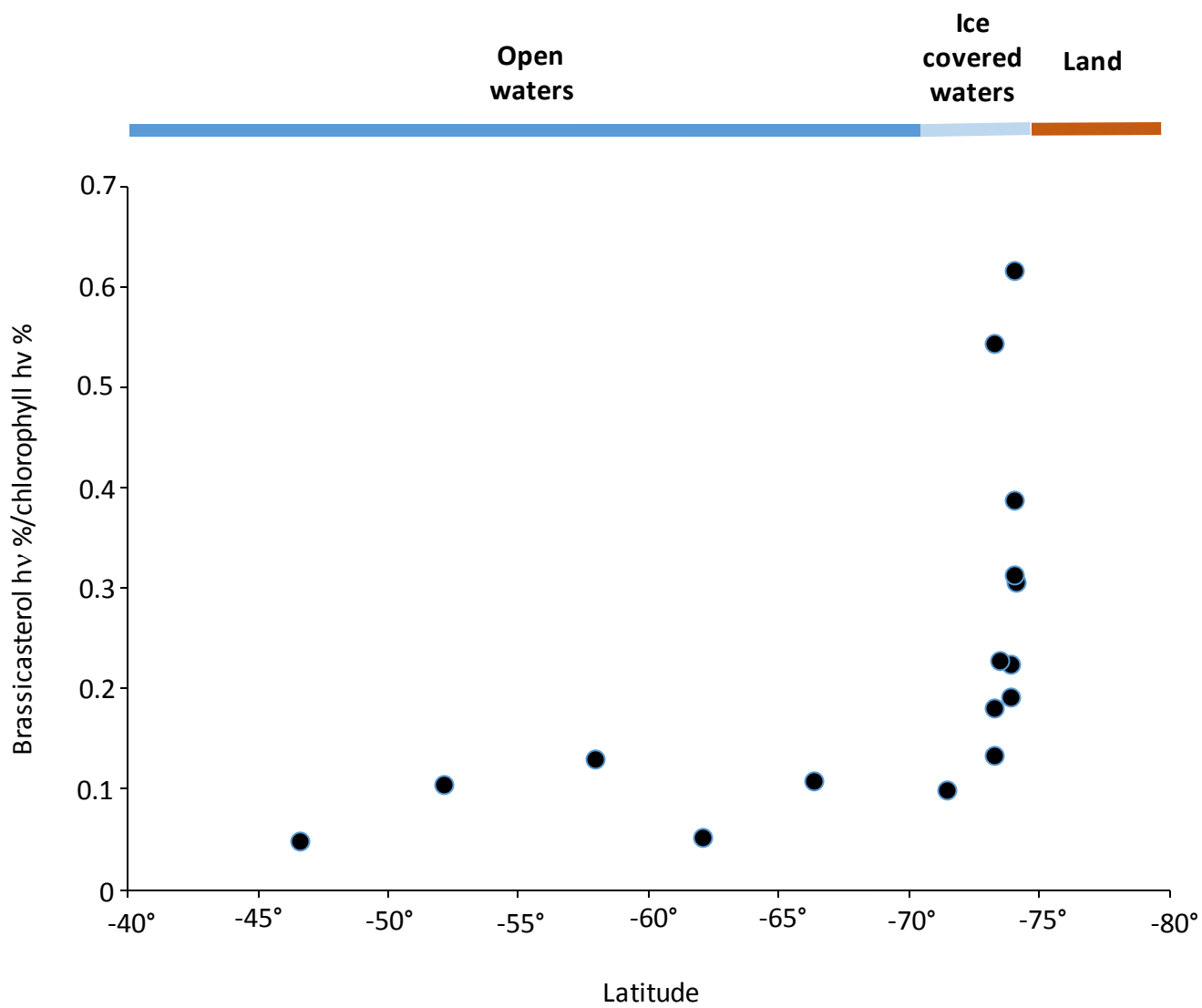
^d Rontani et al., 2012











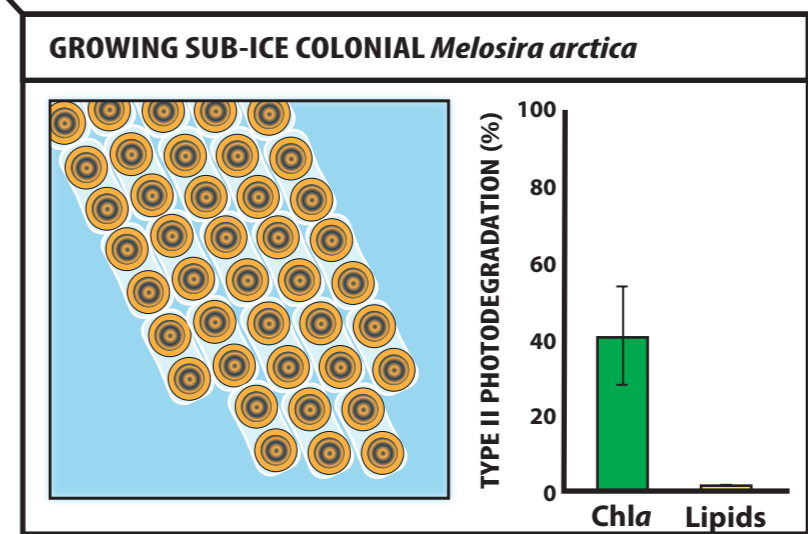
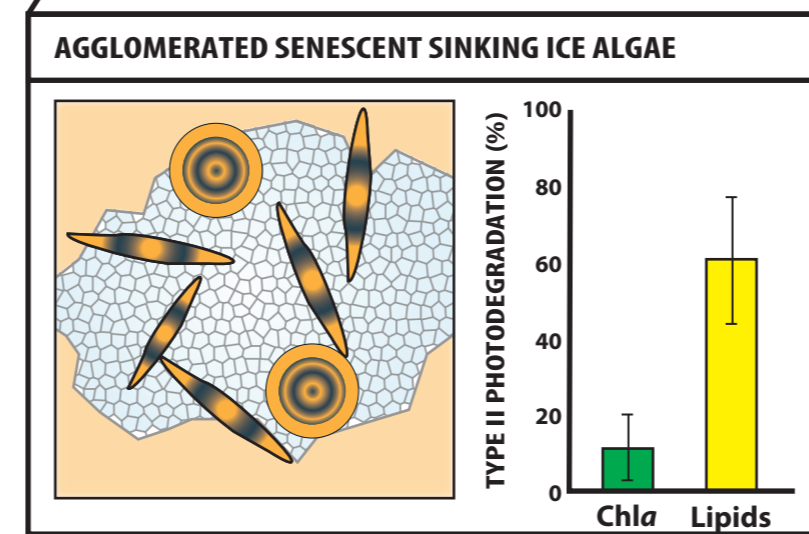
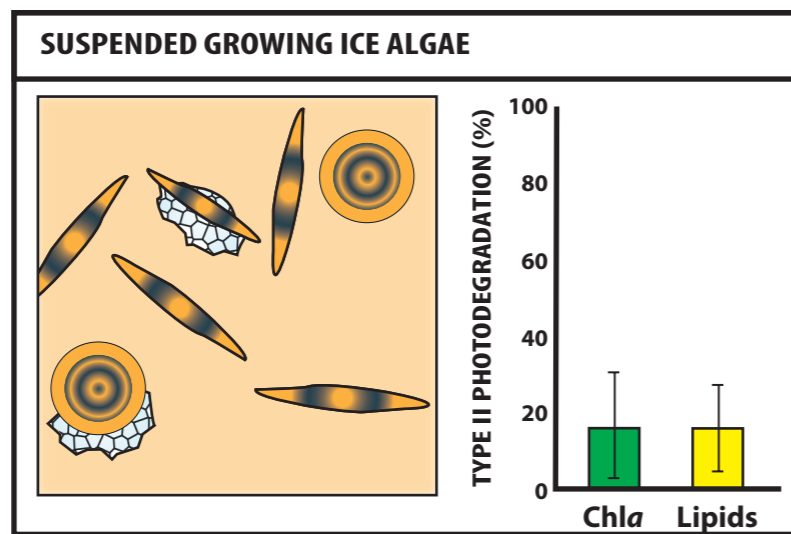
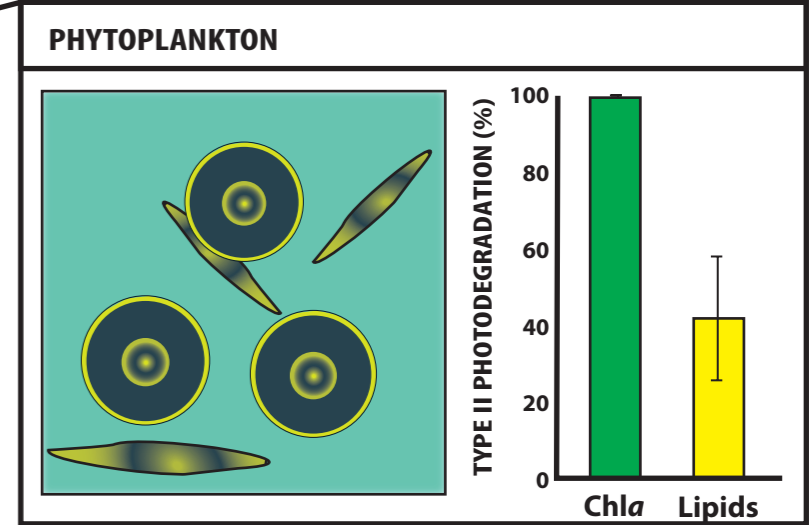
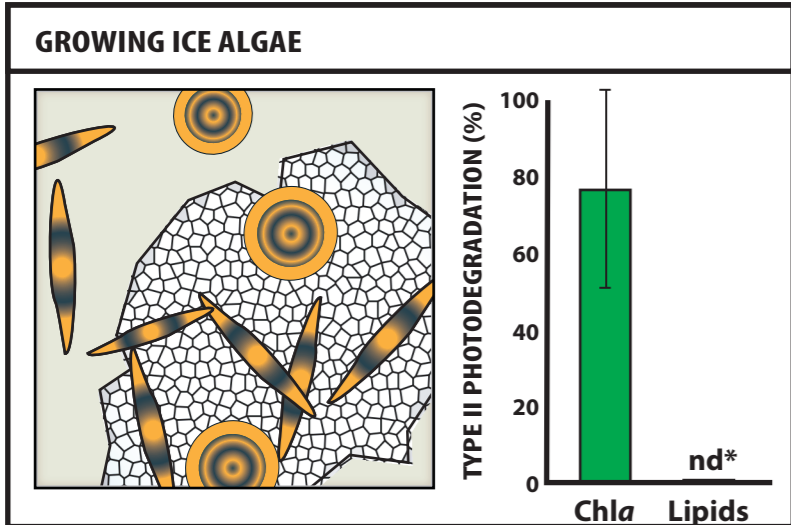
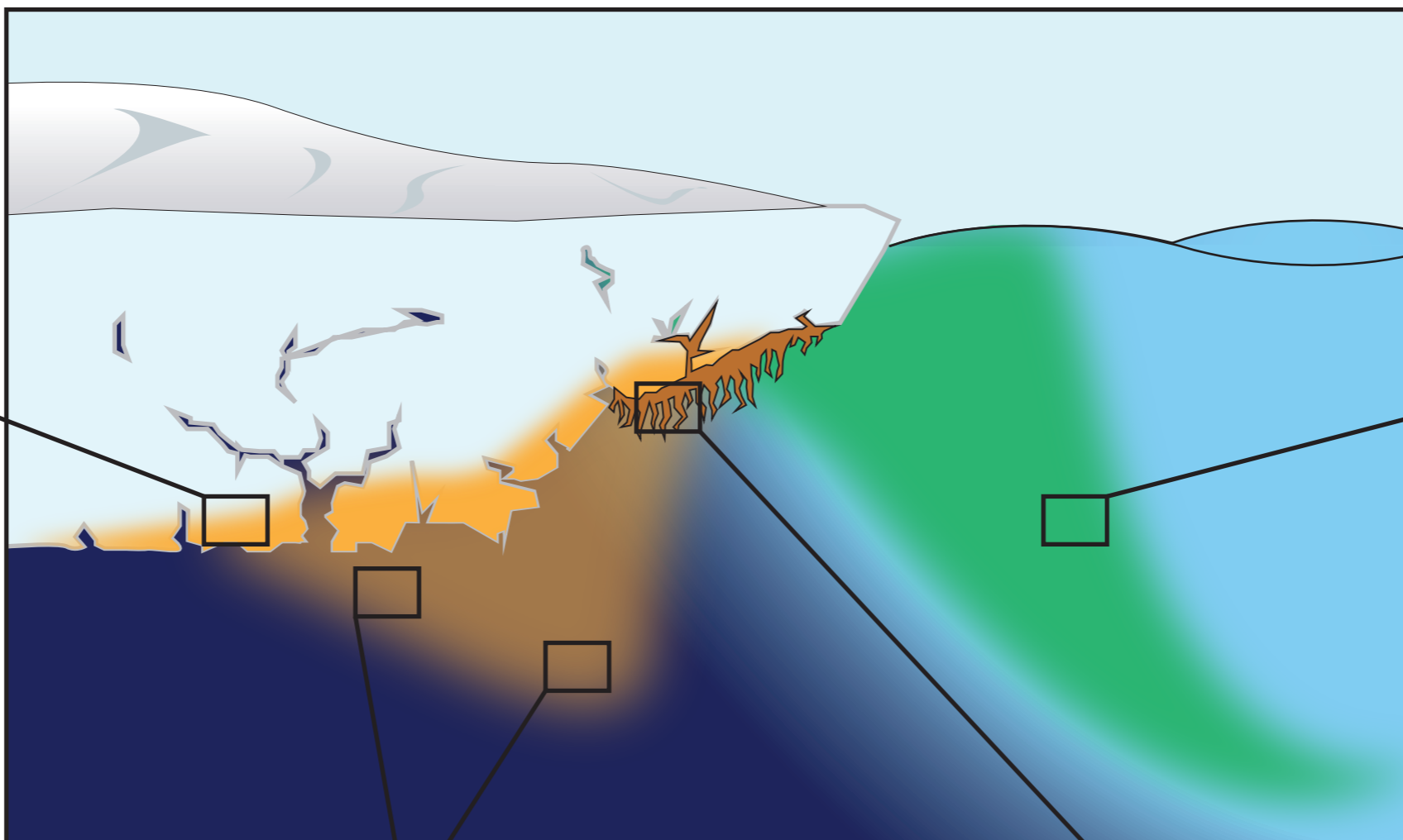


Table S1: Results of Mann – Whitney – Wilcoxon analysis testing the effect of the latitude on the brassicasterol photooxidation percentage : chlorophyll *a* photooxidation percentage ratio. Bold values are indicative of significance.

Source of variation	W	<i>p-value</i>
High latitudes ^a x low latitudes ^b	3861.5	1×10^{-7}
Arctic x Antarctic	583	0.71
Arctic x low latitudes	1107.5	7×10^{-4}
Antarctic x low latitudes	1513	2×10^{-9}

^a Sum of Arctic and Antarctic values

^b Sum of low latitude values (between 67°S and 50°N)

Table S2: Results of Mann – Whitney – Wilcoxon analysis testing the effect of the sample type on the 24-methylenecholesterol photo-oxidation percentage / chlorophyll photo-oxidation percentage, palmitoleic acid photo-oxidation percentage / chlorophyll photo-oxidation percentage and brassicasterol photo-oxidation percentage / chlorophyll photo-oxidation percentage ratios. Bold values are indicative of significance.

Source of variation	24-Me-cholesterol		Brassicasterol		Palmitoleic acid	
	W	<i>p-value</i>	W	<i>p-value</i>	W	<i>p-value</i>
Sea ice x SPM	180	0.4372	212.5	0.5858	4	1.0 x 10⁻⁷
Sea ice x all traps	1	3.0 x 10⁻¹⁰	2	3.7 x 10⁻¹⁰	3	7.2 x 10⁻¹⁰
SPM x all traps	78	3.3 x 10⁻⁶	27	2.0 x 10⁻⁸	242	0.1034
Surface ^a x Traps ^b	79	5.6 x 10⁻¹²	29	7.6 x 10⁻¹⁴	245	1.4 x 10⁻⁶
Traps 5 m x Traps 30 m	10	2.0 x 10⁻⁴	29	0.0225	19	0.0028
Traps 5 m x Traps 100 m	16	2.3 x 10⁻³	0	1.5 x 10⁻⁶	0	1.5 x 10⁻⁶
Traps 30 m x Traps 100 m	0	3.6 x 10⁻⁵	0	7.4 x 10⁻⁷	0	7.4 x 10⁻⁷

^a Sum of sea ice and SPM

^b Sum of traps